# Superposition states at finite temperature

Guillaume Huyet,[1,2] Sonja Franke-Arnold,[1] and Stephen M. Barnett[1]
[1]*Department of Physics and Applied Physics, University of Strathclyde, Glasgow G4 0NG, Scotland*
[2]*Physics Department, National University of Ireland, Cork, Ireland*
(Received 16 May 2000; published 15 March 2001)

We describe a method to create superposition states from a mixed state of a harmonic oscillator. If the initial state is described by a thermal state, then the resulting superposition state will be a ''hot'' superposition state. Such a state can be distinguished from a statistical mixture by its coherence properties. Here we suggest how to demonstrate the coherence of the superposition state by observing interference fringes when the two parts of the wave packet are overlapped. In the case of the mixed superposition state, a partial overlap may not be sufficient to observe the presence of fringes. We introduce therefore the idea of a coherence length for the wave packet and demonstrate its relevance for interferometry of mixed states. We illustrate our ideas with the example of superposition states for the motion of a single trapped ion.

DOI: 10.1103/PhysRevA.63.043812 PACS number(s): 42.50.Dv, 42.65.Ky

## I. INTRODUCTION

Cat states have been the subject of a great interest since Schrödinger's idea of generating a superposition of a macroscopic object [1]. In the original idea a real cat was brought into a superposition of being alive and dead by creating an entanglement of the macroscopic cat with a radioactive particle. This idea has inspired numerous theoretical investigations [2] as such macroscopic superposition states are not observed in classical physics. The difficulty for the creation and the observation of superposition states is mainly due to the fast decay of the coherences [3]. In these studies, superpositions of coherent states of the harmonic oscillator differing by a macroscopic parameter are usually called Schrödinger cats. The two states of the cat are here associated with two coherent states with different mean positions and/or velocities of the harmonic oscillator. These states have been analyzed experimentally in both cavity QED [4] and in ion traps [5]. In cavity QED, the superposition of two coherent states of the field is created by exploiting their entanglement with electronic states of an atom. In the case of an ion trapped by external electromagnetic fields in a harmonic potential, the superposition of two coherent states has been achieved by entangling the motional states with the internal states of the ion.

So far, most of the studies have concentrated on the quantum superposition of two pure states; however, one may also consider the superposition of two mixed cat states, for instance two displaced thermal states [6]. In this wider definition of a cat state, the particle would not be in a superposition of two macroscopically distinct pure states but in a superposition of probability distributions centered around two different phase-space points.

The possibility of creating mixed cat states may also be important from an experimental point of view. In particular, this would allow the realization of mesoscopic quantum states without the requirement of preparing an initial pure state. In the case of trapped ions, this means that cooling to the initial ground state is not necessary to realize a cat state. The initial state could be described by a thermal state and the resulting superposition state will be a ''hot cat'' state. Interestingly, the superposition of two mixed states can also be seen as a mixture of pure superposition states. This concept highlights the importance of the coherence of the motional wave packet. In order to distinguish between a simple mixture of two wave packets and a mixed cat state, one has to probe the coherence between the two wave packets. This may be achieved by causing these wave packets to interfere and measuring the visibility of the resulting interference fringes. In a mixture, the two wave packets are not coherent and thus do not interfere. A pure cat state shows perfect coherence and the interference fringes depend only on the overlap region of the wave packets. In the case of a mixture of cat states, each of the pure states from the statistical mixture generates interference fringes that differ in position, giving rise to a loss of total visibility. In this case, a partial overlap of the two wave packets is not a sufficient criterion for the observation of interference fringes. The interference exhibited by a pure Schrödinger cat state is analogous to optical single mode interference, while that for a hot cat state is more like white-light interference.

In this paper, we first describe the general properties of a mixed cat state and introduce the notion of a coherence length for the harmonically trapped particle. This length can be defined as the normalized root-mean-square width of the squared symmetrically ordered characteristic function of the state. This definition is analogous to that of the optical coherence time in respect to the degree of first-order coherence [7]. We then demonstrate the importance of the coherence length in the analysis of a mixed cat state. We show that the requirement to observe a hot Schrödinger cat for the motion of a trapped ion can be expressed in terms of our coherence length.

## II. PROPERTIES OF CAT STATES

The superposition of two displaced coherent states such as

$$|\Psi_c\rangle = |\alpha_c\rangle + e^{i\theta}|-\alpha_c\rangle, \tag{1}$$

constitutes the usual Schrödinger cat state, provided that the two wave packets are separated in phase space. This implies

 

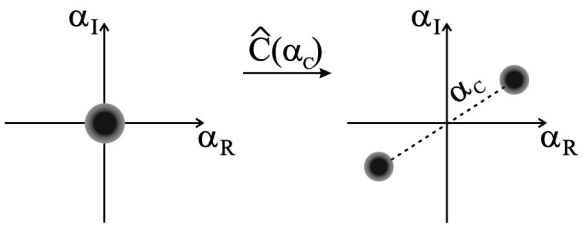


FIG. 1. Schematic representation of the effect of the cat operator $\hat{C}$ onto a wave packet. Note that a proper quantum picture based on a quasiprobability distribution would show interference fringes.

that the distance $|2\alpha_c|$ between the two wave packets has to exceed their width. The given cat state can be mathematically prepared by applying the operator

$$\hat{C}=\hat{D}(\alpha_c)+e^{i\theta}\hat{D}(-\alpha_c), \tag{2}$$

to the vacuum state of the harmonic oscillator, where $\hat{D}(\alpha_c)=\exp(\alpha_c\hat{a}^\dagger-\alpha_c^*\hat{a})$ is the Glauber displacement operator. Figure 1 represents the effect of the operator $\hat{C}$ onto a state centered around $\alpha=0$ in phase space. The operator $\hat{C}$ creates a superposition of the original state described by the density operator $\hat{\rho}$ displaced by $\pm\alpha_c$. The resulting cat state is therefore given by the density operator [8]

$$\hat{\rho}_c=\frac{\hat{C}\hat{\rho}\hat{C}^\dagger}{\mathrm{Tr}(\hat{\rho}\hat{C}^\dagger\hat{C})}. \tag{3}$$

To illustrate the effect of the operator $\hat{C}$, we first consider its action on the vacuum state of the harmonic oscillator $|0\rangle$. The operator $\hat{C}$ transforms this state into the usual Schrödinger cat state described in Eq. (1) with a density operator

$$\begin{aligned}\hat{\rho}_c=&[|\alpha_c\rangle\langle\alpha_c|+|-\alpha_c\rangle\langle-\alpha_c|+|-\alpha_c\rangle\langle\alpha_c|e^{-i\theta}\\&+|\alpha_c\rangle\langle-\alpha_c|e^{i\theta}]/\kappa,\end{aligned} \tag{4}$$

where $|\alpha_c\rangle$ designs the coherent state of the harmonic oscillator and $\kappa=2(1+e^{-2|\alpha_c|^2}\cos\theta)$ is a normalization factor. This can be generalized to cat states generated from any pure state such as Fock or squeezed states. For these states the distance $2|\alpha_c|$ between the two wave packets, which is a characteristic of the cat operator $\hat{C}$ defined in Eq. (2), should strictly be larger than the width

$$\Delta x_\lambda=\sqrt{\mathrm{Tr}(\hat{\rho}\hat{x}_\lambda^2)-\mathrm{Tr}(\hat{\rho}\hat{x}_\lambda)^2}$$

of the initial state, so that there is a superposition of distinct values of $\hat{x}_\lambda$. Here $\hat{x}_\lambda=(\hat{a}e^{-i\lambda}+\hat{a}^\dagger e^{i\lambda})/\sqrt{2}$ represents the quadrature operator for the oscillator. For some states, such as squeezed states, $\Delta x_\lambda$ depends on the direction $\lambda$. In this case, the two wave packets are separated in phase space if $\Delta x_{arg(\alpha_c)}\ll|\alpha_c|$.

If the initial density operator $\hat{\rho}$ describes a mixed state, then the action of the operator $\hat{C}$ creates a mixed cat state as described by the density operator $\hat{\rho}_c$ in Eq. (3). The mixed cat state shares with the pure cat state two characteristic length scales: the distance $\alpha_c$ between the two wave packets and the width $\Delta x_\lambda$ of the initial state. The latter will, in general, have a different value for mixed and pure states.

There is, in addition, a third significant length scale for mixed cat states. This is the coherence length of the wave packet that can be defined in analogy to optics. In optics, the coherence time is the decay time of the first-order coherence or autocorrelation of the electric field. Similarly, the first-order coherence for a harmonic oscillator is defined to be the symmetrically ordered characteristic function [9]

$$\chi(\alpha)=\mathrm{Tr}[\hat{\rho}\hat{D}(\alpha)]. \tag{5}$$

This becomes apparent in the fringe visibility of a single-ion interferometer [10]. Here the visibility of the interference fringes is given by the modulus of the characteristic function in the same way, as the fringe visibility of an optical interferometer is given by the modulus of the first order coherence function. To illustrate the relationship between $\chi$ and an autocorrelation in phase space, we express $\chi(|\alpha|e^{i\lambda})$ as a function of the quadrature operator. For a statistical mixture of the states $|\psi_n\rangle$ with probabilities $P_n$, $\chi(|\alpha|e^{i\lambda})$ can be expressed as

$$\chi(\alpha)=\sum_n P_n\int\psi_n(x_{\arg(\alpha)})\psi_n^*(x_{\arg(\alpha)}-\sqrt{2}|\alpha|)dx_{\arg(\alpha)}. \tag{6}$$

Note that $\chi$ depends on $\lambda$, since $\psi_n(x_\lambda)=\langle x_\lambda|\psi_n\rangle$.

The coherence length of a motional state is related to the symmetrically ordered characteristic function in the same way as the coherence time of the electric field is related to the first order coherence function. Accordingly, we will define the coherence length as

$$\mathcal{L}_\lambda^2=\frac{1}{2}\frac{\int\alpha_\lambda^2|\chi(\alpha)|^2\,d^2\alpha}{\int|\chi(\alpha)|^2\,d^2\alpha}, \tag{7}$$

where $\alpha_\lambda=(\alpha e^{-i\lambda}+\alpha^* e^{i\lambda})/\sqrt{2}$.

It follows from the relation $\alpha\hat{D}(\alpha)=[\hat{a},\hat{D}(\alpha)]$ that

$$\alpha_\lambda\chi(\alpha)=2\,\mathrm{Tr}(\hat{\rho}x_\lambda^2-x_\lambda\hat{\rho}x_\lambda).$$

We can then apply Weyl's theorem [11] to express the coherence length as

$$\mathcal{L}_\lambda^2=\frac{\mathrm{Tr}(\hat{\rho}^2\hat{x}_\lambda^2)-\mathrm{Tr}(\hat{\rho}\hat{x}_\lambda\hat{\rho}\hat{x}_\lambda)}{\mathrm{Tr}\,\hat{\rho}^2}. \tag{8}$$

From this expression, we notice that $\mathcal{L}_\lambda=\Delta x_\lambda$ for any pure state. For a thermal state, $\chi(\alpha)=\exp[-\frac{1}{2}(2\bar{n}+1)|\alpha|^2]$, and the coherence length becomes

$$\mathcal{L}_\lambda=1/\sqrt{2(2\bar{n}+1)}. \tag{9}$$

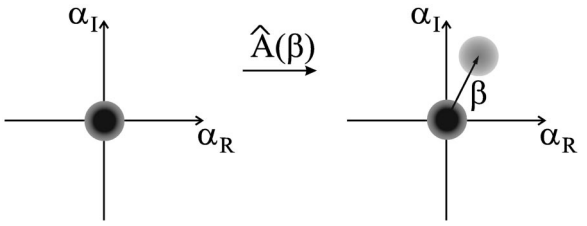


FIG. 2. Schematic representation of the effect of the analyzing operator $\hat{A}$ onto a wave packet. Note that $\phi$ describes the phase difference between the two displaced wave packets and cannot be visualized in this figure.

This indicates that the coherence length decreases as the temperature increases contrary to the width of the wave packet $\sqrt{(2\bar{n}+1)/2}$, which increases with temperature. The coherence length, like the width, depends on the direction $\lambda$. However, we will consider symmetric (unsqueezed) states in the following. For a nonsymmetric state, the same analysis would be valid by taking $\lambda=\arg(\alpha)$.

### III. THE ANALYSIS OF A MIXED CAT STATE

The coherence length, as defined in Eqs. (7) and (8) is an important parameter to demonstrate the successful creation of a mixed cat state since the inequality $\Delta x_\lambda < \alpha_c$ assures the separation but not the coherence between the two wave packets. In analogy with optics, we can probe the coherence between the two wave packets with an interferometer. The observation of fringes then indicates the presence of a superposition state rather than a statistical mixture. An optical interferometer generates two outputs, each of them being in a superposition of two time-delayed wave packets and a measurement of the intensity gives the field autocorrelation. For the cat states, each of the two outputs of the interferometer is a superposition of two coherently shifted wave packets in phase space [10]. The action of the interferometer on the input state can be described by the operator

$$\hat{A}=\frac{1}{2}[1+e^{i\phi}\hat{D}(\beta)], \tag{10}$$

whose effect in phase space is depicted in Fig. 2. Transformations of this kind can be applied to the motional state of a trapped ion [5] or to the field state in a high $Q$ microwave cavity [4] by manipulating the electronic state of an ion or Rydberg atom, respectively.

We apply operator $\hat{A}$ (see Fig. 3) to the cat state $\hat{\rho}_c$ and measure one of the outputs of the interferometer with a probability

$$P(\phi,\beta)=\mathrm{Tr}(\hat{A}^\dagger\hat{\rho}_c\hat{A}) = \frac{1}{2}[1+|\chi_c(\beta)|\cos\{\phi+\arg(\chi_c(\beta))\}]. \tag{11}$$

The state is detected in the second output of the interferometer with a probability $1-P(\phi,\beta)$. Here $\chi_c(\beta)$

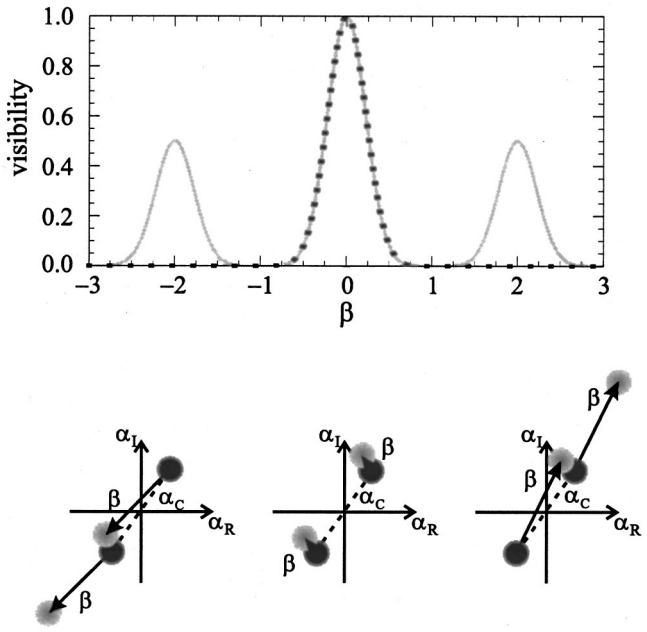


FIG. 3. Top: Visibility of the interference fringes for a hot Schrödinger cat (gray line) and for a statistical mixture (dashed line) for $\beta$ real and with $\bar{n}=2$ and $\alpha_c=2$. Bottom: Schematic representation of the different peaks in phase space. The visibility obtained for a statistical mixture shows only one peak centered at $\beta=0$ corresponding to the total overlap of the wave packets as shown in the center of the lower picture. The visibility for the cat state, however, shows two additional peaks centered at $\beta=\pm 2\alpha_c$ that arise from a partial overlap as indicated on the left and right lower pictures.

$=\mathrm{Tr}[\hat{\rho}_c\hat{D}(\beta)]$ represents the symmetrically ordered characteristic function of the cat state that can be written as

$$\chi_c(\beta)=\{\chi(\beta)[e^{\alpha_c^*\beta-\alpha_c\beta^*}+e^{-\alpha_c^*\beta+\alpha_c\beta^*}]+\chi(\beta+2\alpha_c)e^{-i\theta} +\chi(\beta-2\alpha_c)e^{i\theta}\}/[2+\{e^{-i\theta}\chi(2\alpha_c) +e^{i\theta}\chi(-2\alpha_c)\}]. \tag{12}$$

The visibility of the interference fringes of the probability (11) is then given by the modulus of this function. If the state $\hat{\rho}_c$ was not a cat state but a mixture of two displaced wave packets described by

$$\hat{\rho}_{nc}=\frac{1}{2}[\hat{D}(\alpha)\hat{\rho}\hat{D}(-\alpha)+\hat{D}(-\alpha)\hat{\rho}\hat{D}(\alpha)], \tag{13}$$

then the visibility would be

$$V(\beta)_{nc}=\frac{1}{2}|\chi(\beta)[e^{\alpha^*\beta-\alpha\beta^*}+e^{-\alpha^*\beta+\alpha\beta^*}]|. \tag{14}$$

This function takes its maximum value of one at $\beta=0$ and is proportional to the modulus of the characteristic function of the initial state as shown in Fig. 3. The width of $V(\beta)_{nc}$ is given by the coherence length of the initial state as defined in Eq. (7). The observed fringes are similar to those

observed in optical interferometry with white light when the two paths of the interferometer have approximately the same length.

For a Schrödinger cat state the displacement $\alpha_c$ is larger than the coherence length and the visibility contains three maxima, centered at $\beta=0$ and $\pm 2\alpha_c$ as indicated by the solid line in Fig. 3. The peak observed at $\beta=0$ is the same as for the non-cat-state and is not an intrinsic feature of a cat state. The visibility of the peaks centered at $\beta=\pm 2\alpha_c$ is given by

$$V(\beta)\simeq\frac{1}{2}|\chi(\beta\mp 2\alpha_c)|. \tag{15}$$

These peaks arise from the overlap of one part of the wave packet with the other part of the displaced wave packet. Their presence, therefore, demonstrates the coherence between the two wave packets and is a characteristic of a Schrödinger cat. Accordingly, the visibility at these secondary peaks is one-half and their width is the coherence length as for the central peak. The fact that the secondary peaks have the same width as the central peak may be important for the experimental observation of a mixed Schrödinger cat with an unknown coherence length. If the central peak is resolved and there is no secondary peak, then the state is a statistical mixture. Interestingly, the decay of these secondary peaks could be used to study the decoherence of a hot cat.

## IV. HOT CAT STATE FOR THE MOTION OF A TRAPPED ION

Schrödinger cats have been realized experimentally by preparing a single trapped ion in a superposition of two spatially separated wave packets [5]. This was achieved by entangling the motional state of the ion with its electronic states. The ion was first cooled to its motional and electronic ground states $|\psi\rangle=|0\rangle|-\rangle$, where $\pm$ represents the ground and the excited states of the atom, while $|0\rangle$ is the vacuum state. The wave packet was then split into its ground and excited state by a $\pi/2$ pulse, using a Raman transition (via a third level) two-photon resonant with the transition from $|-\rangle$ to $|+\rangle$. This creates the state

$$\frac{|0,-\rangle-ie^{i\phi}|0,+\rangle}{\sqrt{2}}. \tag{16}$$

The excited part of this state was then displaced in phase space by applying a Raman transition between two motional levels of the excited state, so that the state was transformed into

$$\frac{|0,-\rangle-ie^{i\phi}\hat{D}(\alpha)|0,+\rangle}{\sqrt{2}}, \tag{17}$$

with $\alpha=\eta\Omega_d\tau e^{-i\phi}$. Here $\eta$ is the Lamb-Dicke parameter, $\Omega_d$ denotes the coupling strength of the displacement beam, $\tau$ is the duration of the pulse and $\phi$ is the phase difference between the two Raman beams [12]. The population of excited and ground state was then exchanged via a $\pi$ pulse in order to generate the state

$$\frac{|0,+\rangle-ie^{i\phi}\hat{D}(\alpha)|0,-\rangle}{\sqrt{2}}. \tag{18}$$

Finally, the excited state was displaced by an amount of $-\alpha$ and a $\pi$ pulse at the carrier frequency generates the state

$$\frac{1}{\sqrt{2}}[\hat{D}(-\alpha)|0,-\rangle-ie^{i\phi}\hat{D}(\alpha)|0,+\rangle]. \tag{19}$$

To analyze this state, a $\pi/2$ pulse was applied and the probability of the ion being in the ground state was measured. The presence of interference fringes then showed the existence of a superposition rather than a statistical mixture.

With another method, proposed in Ref. [13], Schrödinger cats could be obtained by sending two $\pi/2$ laser pulses in the strong excitation regime. In this regime, a $\pi/2$ pulse travelling toward the positive $x$ altered the wave function of an ion in a pure motional state $|s\rangle$ and in its electronic states $|\pm\rangle$ as

$$|s,\pm\rangle\rightarrow|s,\pm\rangle\pm ie^{\mp i\theta}\hat{D}(\mp i\eta)|s,\mp\rangle. \tag{20}$$

Here $\theta$ is the phase difference between the two Raman pulses constituting the $\pi/2$ pulse. The effect of a $\pi/2$ pulse traveling in the negative-$x$ direction can be calculated by changing $\eta$ to $-\eta$. We note that, due to the oscillation of the ion in the trapping potential, the effect of a pulse traveling toward the negative $x$ sent at the time $t=0$ is the same as the effect of a pulse traveling toward the positive $x$ sent at time $t=\pi/\nu$, where $\nu$ is the trapping frequency. Most ion-trap experiments are run in the Lamb-Dicke regime, where $\eta$ is a small parameter that limits the possible displacement per light pulse. It is possible, however, to reach large values of $\eta$ by applying sequences of $\pi$ pulses [13]. The formula (20) can therefore be extended to large values of $\eta$.

To create a Schrödinger cat from the pure motional state $|s,-\rangle$, one applies two $\pi/2$ pulses from opposite directions with a time delay of a multiple of the period of the trap, see right of Fig. 4. The ion is then in a superposition of four states; two associated with the electronic ground state and two with the excited state. By measuring the ground-state probability with the usual quantum jump technique [14], the wave function is projected onto the excited state if no fluorescence is observed. Otherwise, the wave function is destroyed and the experiment has to be restarted. With this method the following Schrödinger cat state is generated,

$$[\hat{D}(i\eta e^{-i\varphi})+e^{-i\theta_C}\hat{D}(-i\eta e^{-i\varphi})]|s,+\rangle. \tag{21}$$

Here $\theta_C=\theta_2-\theta_1$ is the phase difference between the second and the first laser pulse and the phase $\varphi=\nu t$ results from the evolution of the cat state after its creation.

Neither of the methods presented above involves the phonon number of the initial motional state of the ion. They can therefore be generalized to arbitrary motional states, including thermal states. However, ''hot'' cat states can be more

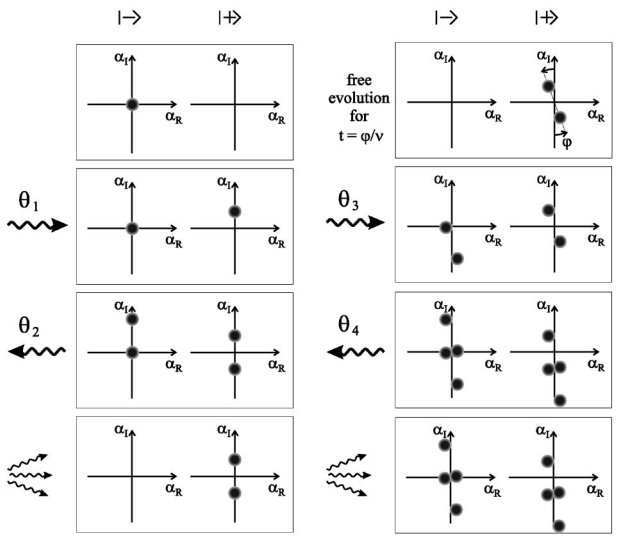


FIG. 4. At the left the creation of a Schrödinger cat state in the strong excitation regime is indicated. For this two $\pi/2$ Raman pulses from opposite directions are followed by the detection of the ground state probability and subsequent collapse into the cat state. The right part of the figure shows the pulse sequence with which the cat state can be analyzed.

difficult to observe than pure cat states as their coherence length decreases with temperature. In the following we introduce a method to analyze a general Schrödinger cat state, employing the strong excitation regime. As both methods are mathematically very similar, the results can be extended also to the method employing the weak excitation regime used in [5].

The analysis of the cat state (21) involves a similar pulse sequence as the one used for its creation, described above. We also introduce a varying mismatch in the timing of the next laser pulse in order to analyze the precision required for the observation of a mixed cat state. After the time $\varphi/\nu$, the third pulse is sent and a fourth pulse traveling in the opposite direction is applied after the period $2\pi n/\nu$. The wave function is therefore split into eight wave packets, four being in the ground state and four in the excited state.

$$|\psi\rangle = |\psi_+\rangle|+\rangle + |\psi_-\rangle|-\rangle \tag{22}$$

with

$$|\psi_+\rangle = \hat{D}(i\eta)[e^{-i\theta_q}\hat{D}(a) + e^{i(\Theta-\theta_C)}\hat{D}(-ib) - e^{i(\Theta+\theta_A)}\hat{D}(ib) - e^{i(\theta_A-\theta_C-\Theta)}\hat{D}(-a)]|s\rangle,$$

$$|\psi_-\rangle = -ie^{-i\theta_4}[e^{-i\Theta}\hat{D}(a) + e^{i(\theta_A+\Theta)}\hat{D}(ib) + e^{-i\theta_C+\Theta}\hat{D}(-ib) + e^{i(\theta_A-\theta_C-\Theta)}\hat{D}(-a)]|s\rangle.$$

Here $\theta_A = \theta_4 - \theta_3$ is the phase difference between the last two laser pulses and we use the phase $\Theta = \eta^2 \sin\varphi$ and the displacement parameters $a = 2\eta e^{-i\varphi/2}\sin\varphi/2$, $b = 2\eta e^{-i\varphi/2}\cos\varphi/2$. The probability that a measurement will show the ion to be in its ground state is

$$P_- = \frac{\langle\psi_-|\psi_-\rangle}{\langle\psi_+|\psi_+\rangle + \langle\psi_-|\psi_-\rangle}. \tag{23}$$

In order to have a macroscopic separation of the two wave packets of the cat state, we need to assume that the width $\Delta x_\lambda$ of the state $s$ is much smaller than $\eta$, and consequently terms like $\langle s|\hat{D}(\eta)|s\rangle$ can be neglected compared to 1. A perfect overlap of the two wave packets is achieved only if $\varphi$ is a multiple of $\pi$ and we will find a non vanishing visibility of the interference fringes only in the vicinity of $\varphi \approx n\pi$. In this regime we can linearize the geometrical functions of the displacement parameters $a$ and $b$ and we find

$$P_- = \frac{1}{2}\left[1 + \frac{1}{2}\mathrm{Re}[\langle s|\hat{D}(2a)|s\rangle e^{i(\theta_C-\theta_A)}]\right]. \tag{24}$$

The visibility of the resulting interference fringes is then given by

$$V = \frac{1}{2}|\langle s|\hat{D}(2a)|s\rangle|, \tag{25}$$

which is the modulus of the characteristic function of the motional state $|s\rangle$.

In the following, we investigate the analysis of different motional states and, in particular, of mixed states. The previous calculation may also be applied to a density operator $\rho$ formed as a statistical mixture of the pure motional states $|\psi_n\rangle$ with probabilities $P_n$,

$$\rho = \sum_{n=0}^{+\infty} P_n |\psi_n\rangle\langle\psi_n|.$$

If a Schrödinger cat state is created from such a mixed state and then analyzed by its interference, then the visibility of the interference fringes is given by

$$V = \frac{1}{2}\left|\sum_{n=0}^{+\infty} P_n\langle\psi_n|\hat{D}(2|a|)|\psi_n\rangle\right| \tag{26}$$

We mentioned earlier that a Schrödinger cat state generated from a thermal state can be understood as a thermal mixture of Schrödinger cat states generated from Fock states. This is reflected in the coherence properties of the cat state. The visibility of a thermal cat state is given by a thermal mixture of the visibilities of the different Fock states [Eq. (26)].

In order to illustrate this, we first consider a cat state that is generated from the $n$th Fock state of the motion. The visibility of its interference fringes can be calculated to be

$$V_n = \frac{1}{2}e^{-2\eta^2\varphi^2}|L_n(4\eta^2\varphi^2)|, \tag{27}$$

where $L_n$ is the $n$th Laguerre polynomial and we used the fact that $\langle n|\hat{D}(\alpha)|n\rangle = \exp(-|\alpha|^2/2)L_n(|\alpha|^2)$. As the accumulated phase $\varphi$ between creation and analysis of the state is varied, $2n+1$ maxima are observed. These correspond to the possible overlaps of the two wave packets, each having $n$

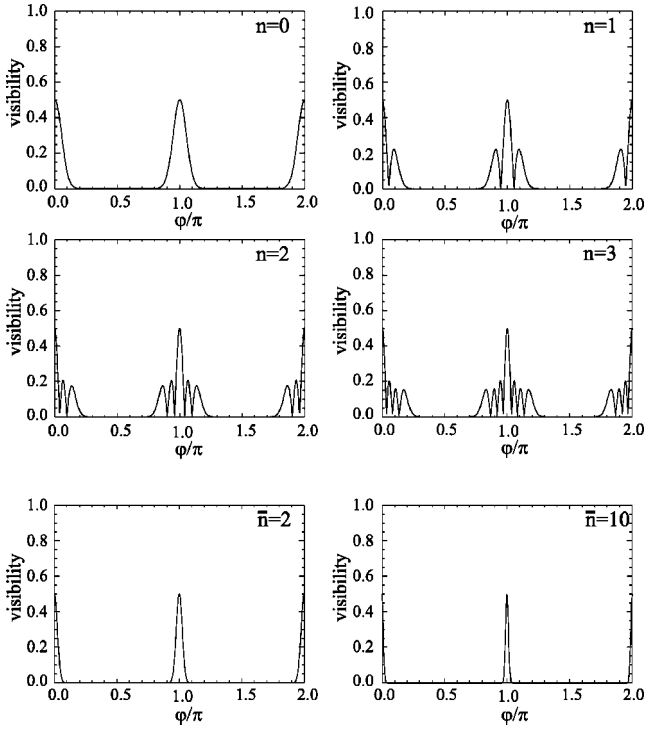


FIG. 5. The visibility of the interference fringes for Schrödinger cat states generated from the Fock states $|0\rangle$, $|1\rangle$, $|2\rangle$, and $|3\rangle$ shows $n+1$ maxima (top). For thermal states the side peaks of the visibility average out and the width of the central peak decreases with increasing $\bar{n}$ (bottom). For the calculation we assumed $\eta=3$ and $\theta_C=\pi/2$.

$+1$ maxima. The width of these side peaks is decreasing with increasing $n$. The visibility of the zeroth to third Fock state as a function of the delay $\varphi$ is shown in the upper part of Fig. 5.

An initial thermal state can be considered as a mixture of the different Fock states weighted with the thermal distribution and the visibility in this case becomes

$$V=\frac{1}{2}\exp[-2\eta^2(2\bar{n}+1)\varphi^2]. \tag{28}$$

As the side peaks of the different Fock states occur at different values of the phase $\varphi$, they average out in the thermal distribution. Interference fringes occur only if $\varphi$ is an integer multiple of $\pi$ (see lower part of Fig. 5). The width of these remaining maxima decreases with increasing temperature as $1/\sqrt{2\sim\bar{n}+1}$.

A somewhat similar situation occurs for optical white-light interferometry, where the visibility of interference fringes depends crucially on the difference in the path length of the two interferometer arms. The broader the frequency distribution, the more accurately the optical path lengths must match in order to see interference. In other words, the allowed mismatch is directly related to the coherence time of the light source.

In the analysis of thermal Schrödinger cat states, the full width at half maximum of the visibility can be expressed via the coherence length as

$$\Delta\varphi_{\mathrm{FWHM}}=\frac{\ln 2}{\eta\sqrt{2\bar{n}+1}}=\frac{\sqrt{2}\ln 2}{\eta}\mathcal{L}_\lambda . \tag{29}$$

This shows that the detection of a ''hot'' Schrödinger cat state requires a timing mismatch of less than the corresponding coherence length. As the coherence length decreases with increasing average motional quantum number [see Eq. (9)], the required precision in the timing of the analyzing pulses rises with the temperature of the hot cat state.

We point out that for simplicity we have assumed a perfect timing between the two pulses that constitute the generation and analysis of the cat state, and have investigated only a mismatch in the delay between those sets of pulses. However, the required precision in the timing of all pulses depends on the coherence length and therefore on the temperature of the initial motional state.

## V. CONCLUSION

We have shown that mixed Schrödinger cat states can be generated from single-trapped ions in arbitrary motional states, and in particular from thermal states. In contrast to existing schemes, this allows the realization of mesoscopic quantum states without the requirement of first cooling the ion down to the motional ground state. We have provided a method to distinguish between mixed Schrödinger cat states and mixtures of two displaced wave packets by examining their coherence properties. In analogy with the optical-coherence time, a coherence length was defined as a measure for the coherence of matter waves. For thermal states of ions, the coherence length decreases with temperature and thus makes the detection of ''hot'' Schrödinger cat states more difficult. In particular, the allowed mismatch in the timing of the analysis of the Schrödinger cat was shown to be proportional to the coherence length of the original wave packet. This places greater restrictions on the accuracy required to analyze hot cat states.

The possibility to create hot Schrödinger cat states allows us to explore superpositions of increasingly macroscopic objects. We believe that the coherence length will play an important role in describing these superpositions.

## ACKNOWLEDGMENTS

We thank Professor Rainer Blatt for first asking us about superpositions of mixed states and for his helpful advice. This work was supported by the TMR program of the Commission of the European Union through the Quantum Structures Network.

[1] E. Schrödinger, Naturwissenschaften **23**, 807 (1935).
[2] V. Buzek and P.L. Knight, in *Progress in Optics*, edited by E. Wolf (North-Holland, Amsterdam, 1995), Vol. XXXIV, p. 1, and references therein.
[3] D.F. Walls and G.J. Milburn, Phys. Rev. A **31**, 2403 (1985).
[4] M. Brune, E. Hagley, J. Dreyer, X. Matre, A. Maali, C. Wunderlich, J.M. Raimond, and S. Haroche, Phys. Rev. Lett. **77**, 4887 (1996).
[5] C. Monroe, D.M. Meekhof, B.E. King, and D.J. Wineland, Science **272**, 1131 (1996).
[6] K. Zhu, H. Tang, C. Li, D. Huang, and X. Li, J. Mod. Opt. **43**, 323 (1996).
[7] M. Born and E. Wolf, *Principles of Optics* (Pergamon Press, Oxford, 1980).
[8] This transformation has the form of an operation on the density matrix, K. Kraus, *States Effects and Operations*, Lecture Notes in Physics Vol. 190 (Springer-Verlag, Berlin, 1983).
[9] This function allows us to obtain the moments of any chosen operator by differentiation and the Wigner function by Fourier transform. See, for example, S.M. Barnett and P.M. Radmore, *Methods in Theoretical Quantum Optics* (Oxford University Press, Oxford, 1997), p. 106.
[10] P.J. Bardroff, M.T. Fontenelle, and S. Stenholm, Phys. Rev. A **59**, R950 (1999).
[11] P. Marian and T.A. Maurian, Phys. Rev. A **47**, 4474 (1993), and references therein.
[12] Similar Raman pulse sequences were applied in experiments described in the following papers: D. Leibfried, D.M. Meekhof, B.E. King, C. Monroe, W.M. Itano, and D.J. Wineland, Phys. Rev. Lett. **77**, 4281 (1996); D. Leibfried, D.M. Meekhof, C. Monroe, B.E. King, W.M. Itano, and D.J. Wineland, J. Mod. Opt. **44**, 2485 (1997).
[13] J.F. Poyatos, J.I. Cirac, R. Blatt, and P. Zoller, Phys. Rev. A **54**, 1532 (1996).
[14] The detection efficiency for the electronic states is almost 100%, see W. Nagourney, J. Sandberg, and H. Dehmelt, Phys. Rev. Lett. **56**, 2797 (1986); Th. Sauter, W. Neuhauser, R. Blatt, and P.E. Toschek, *ibid.* **57**, 1696 (1986); J.C. Bergquist, R.G. Hulet, W.M. Itano, and D.J. Wineland, *ibid.* **57**, 1699 (1986).